

Extreme load estimation of the wind turbine tower during power production

Wind Engineering

1–14

© The Author(s) 2019

Article reuse guidelines:

sagepub.com/journals-permissions

DOI: 10.1177/0309524X19872766

journals.sagepub.com/home/wie

Atsushi Yamaguchi¹, Prasanti Widyasih Sarli and
Takeshi Ishihara

Abstract

Wind turbines have to be designed against extreme load during power production with the recurrence period of 50 years. This extreme load is usually calculated through statistical extrapolation. However, large uncertainties exist in the estimation of the extreme load. This study aims to reduce these uncertainties in the statistical extrapolation by using systematic simulations. First, a new criterion is proposed for the data sets to be used for the statistical extrapolation and the resulting uncertainty satisfies the requirement in the standard for prediction of wind load. Then, a new extrapolation factor for load extrapolation is proposed and the predicted maximum tower bending moments at all the heights show favorable agreement with measurement. Finally, empirical formulae are proposed to estimate the expected value of the maximum tower bending moment and the predicted values show good agreement with the numerical simulations.

Keywords

Extreme load during power production, statistical extrapolation, convergence criteria, extrapolation factor, empirical formulae for tower maximum load estimation

Introduction

Wind turbines have to be designed against extreme load during power production with the recurrence period of 50 years as specified in IEC61400-1:2005 + AMD1:2010 (2010) for design load case 1.1 (DLC 1.1). This extreme load is usually calculated through statistical extrapolation in which the 50 years load is estimated from limited number of 10-min simulations.

The statistical extrapolation may result in uncertainties in the estimation of the extreme load. As shown by Moriarty (2008), different packs of the simulations can result in different estimations. These uncertainties can be controlled by the convergence criteria developed by Fogle et al. (2008). However, it is not clear whether these criteria are enough or not to satisfy the level of the uncertainty assumed in the partial safety factor for extreme load (Tarp-Johansen et al., 2002).

As an alternative to the load extrapolation, IEC61400-1 also provides a simple method for the extreme load estimation, which is to multiply a constant extrapolation coefficient of 1.5 to the expected value of the 10-min maximum load. However, the use of the constant coefficient may underestimate or overestimate the extreme load. In order to improve this overestimation, Ishii and Ishihara (2010) developed an empirical extrapolation coefficient as a function of turbulence intensity and annual mean wind speed based on the numerically simulated fore-aft tower base moment. The applicability of this factor to the other component of tower is questionable because the factor can be different depending on the components as shown by Moriarty (2008).

Ishii and Ishihara (2010) also developed empirical formulae to estimate the expected value of the 10-min maximum load to avoid complex simulation of the wind turbine assuming that the tower base moment is caused by the

The University of Tokyo, Tokyo, Japan

Corresponding author:

Atsushi Yamaguchi, The University of Tokyo, 7-3-1 Hongo, Bunkyo, Tokyo 113-8656, Japan.

Email: atsushi@bridge.t.u-tokyo.ac.jp

thrust force on the rotor, and the drag force on the nacelle and the tower. However, at the tower top, the effect of rotor moment on the tower bending moment is not negligible and it might underestimate the extreme load at the tower top.

Numerical model used in this study and its validation by the field test are described in “Numerical model and validation” section. A new criterion and a new extrapolation factor are then proposed to reduce the uncertainty in the statistical extrapolation in “A new convergence criterion” and “A new extrapolation factor” sections. Finally, empirical formulae are proposed to estimate the expected value of the maximum moment at all the positions of the tower and are validated by the numerical simulations in “Empirical formulae for the expected maximum tower load estimation” section.

Numerical model and validation

In this study, an offshore wind turbine at Choshi Offshore Demonstration Project (Fukumoto et al., 2013) is used to validate the numerical model. This wind turbine is installed on a gravity foundation, and wave load on the tower is negligible since wave hardly reaches the tower. “Field measurement at Choshi demonstration site” section describes the field measurement at Choshi demonstration site. Wind turbine model and its validation are presented in “Wind turbine model and validation” section.

Field measurement at Choshi demonstration site

Figure 1 shows the 2.4 MW wind turbine at Choshi demonstration site. Strain gauges are installed on the tower shell at 73.1 and 10.9 m above sea level as shown in Figure 1. Four strain gauges are installed at each height to measure the vertical strain. The initial offset of the strain gauges are calibrated by using the measured strain data during nacelle rotation test in which the nacelle-yaw angle is rotated 360° while wind turbine is in parked condition. The data were sampled at 50 Hz frequency and statistics are calculated for each 10 min. The supervisory control and data acquisition (SCADA) data of the wind turbine are also stored to record the operation status, pitch angle, rotor speed, and generated power at 1-s sampling frequency (Okubo et al., 2016).

To the east of the turbine, a met mast is installed to measure the wind characteristics. These data are used to model the wind for the validation. To investigate the characteristic of the turbulence, the bin average of the turbulence intensity for the whole range of wind speed from cut-in to cut-out was calculated in an increment of 1 m/s.

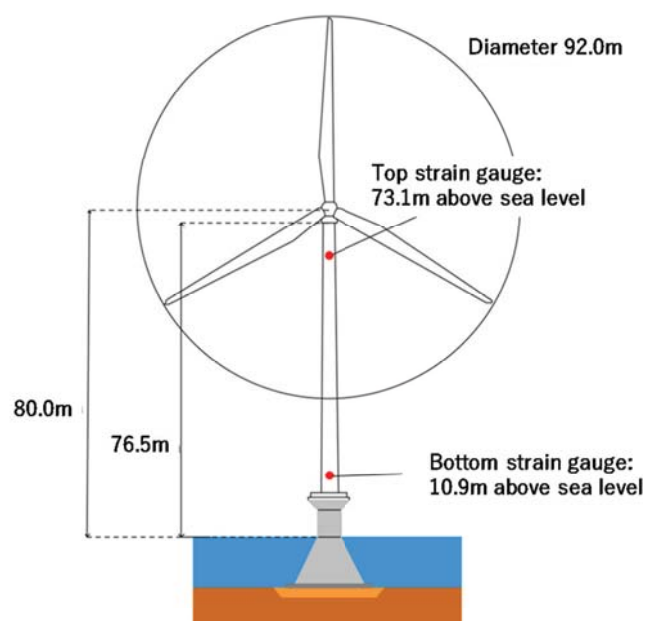


Figure 1. Wind turbine of 2.4 MW at Choshi demonstration site.

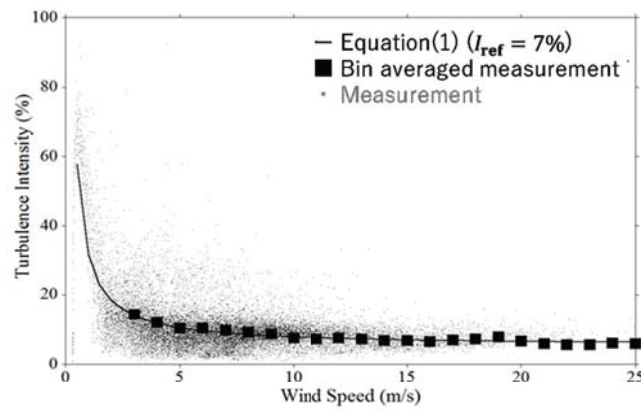


Figure 2. Measured turbulence intensity at the hub height at the observation mast.

Table 1. The dimensions and weight of the nacelle, hub, rotor, and the tower.

Dimension of the nacelle	10.8 m (length) × 4.0 m (width) × 7.7 m (height)
Mass of the nacelle	110,000 kg
Length of the blade	44.7 m
Mass of the rotor	58,728 kg
Hub height	80 m
Diameter of the tower	4 m (bottom)/3 m (top)
Shell thickness of the tower	38 mm (bottom)/22 mm (top)
Damping ratio of the tower	0.2% (first mode) and 2.4% (second mode)

Then, an approximation of the turbulence intensity distribution with wind speed was attempted by using the equation proposed in IEC 61400-1

$$I_1 = \frac{I_{\text{ref}}(0.75V + b)}{V} \quad (1)$$

Here, I_{ref} is the expected value of turbulence intensity at 15 m/s and V is the wind speed. b is set to 3.75 m/s to represent the 50% quantile. By using least square fitting of the bin-averaged turbulence intensity, I_{ref} was identified as 7%. Figure 2 shows the measured turbulence intensity and bin-averaged value together with the estimated 50% quantile by using equation (1).

Four months of the strain data are used to estimate the fore-aft tower bending moment. The data are divided into sets of 10-min data, and mean, maximum, and standard deviation are calculated for all the 10 min. Only such data where the wind turbine is in operation for all the 10 min are used for the validation.

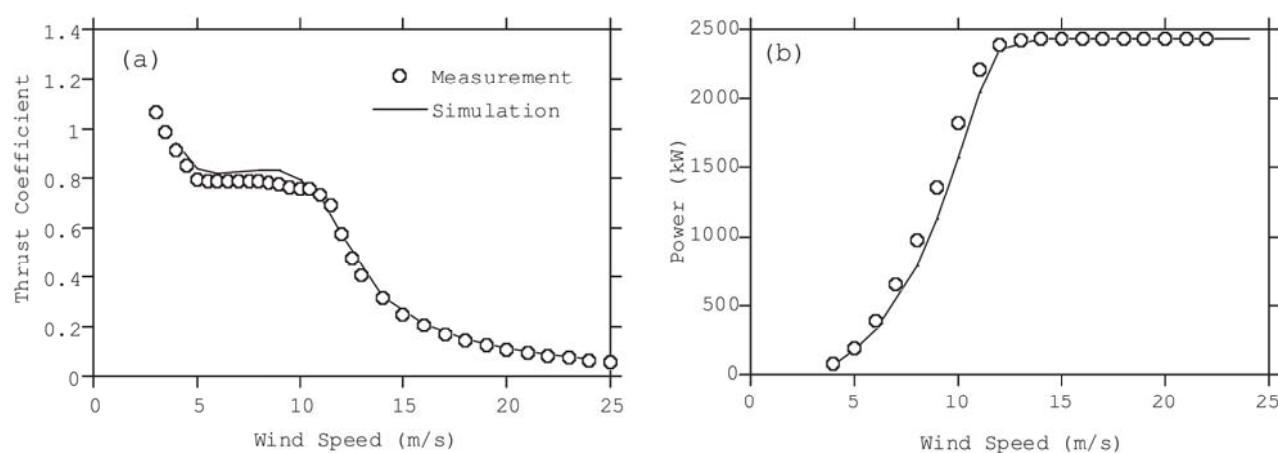
Wind turbine model and validation

A wind turbine model was built by using GH Bladed 4.4 (DNV-GL, 2010) to simulate the wind loads during power production. The dimension and weight of the nacelle, hub, and the tower are shown in Table 1. The wind turbine has a conventional variable speed and a variable blade-pitch-to-feather configuration, and the control parameters are based on the model proposed by Yoshida (2011), which are shown in Table 2. The nacelle-yaw angle control is not activated, and no yaw misalignment is assumed. The aerodynamic properties of the blade are based on the Japan Society of Civil Engineers (JSCE) guideline (Ishihara, 2010). The modal damping ratios of the first and second tower modes are based on the measurement carried out by Oh and Ishihara (2018).

To investigate the response of the wind turbine to different wind speeds, simulations are run from the cut-in wind speed of 4 m/s to the cut-out wind speed of 24 m/s with an increment of 1 m/s. At each wind speed, 35 different random turbulence seeds are used to generate different wind fields. Wind shear is set to 0.14 based on IEC 61400-1, whereas the Mann model was used to generate the turbulence (DNV-GL, 2010).

Table 2. Summary of control parameters.

Rated power	2437 kW
Minimum generator speed	690 r/min
Rated generator speed	1150 r/min
Rated generator torque	21,087.7 Nm
Optimal torque control gain	0.556 N m/(rad/s ²)
Torque control proportional gain	750.67
Torque control integral gain	170
Pitch control proportional gain	0.018884
Pitch control proportional gain	0.008226
Gain scheduling for pitch control	Yoshida (2011)

**Figure 3.** (a) Thrust curve and (b) power curve of the wind turbine.

Power and thrust coefficient for different wind speed are calculated by using the described model and compared with the bin average value of the measurements as shown in Figure 3. The simulations show good agreements with the measurements. Figure 4 shows the comparison of mean, standard deviation, and maximum of the fore-aft tower bending moment at two different heights. The measurement data are the bin average of 10 min mean, standard deviation, and maximum for 4 months while the simulation results are the average of 10 min mean, standard deviation, and maximum for 35 different simulations with different turbulent wind field with different random seeds. The simulation results give good agreements with the measurements.

Extreme load estimation

The extreme load during power production is investigated by using the numerical model validated in “Numerical model and validation” section. Two different turbulence intensity levels ($I_{\text{ref}} = 12\%$ and 16%) and four different annual mean wind speeds ($\bar{U} = 7, 8, 9$, and 10 m/s) at the hub height are used, and extreme load during power production is estimated for each case. At least 35, 10-min load simulations are carried out for each turbulence level and wind speed between cut-in and cut-out with the interval of 1 m/s as recommended by IEC 16400-1. When the convergence criteria were not satisfied, the number of simulation is doubled until the criteria are satisfied. Rayleigh distribution is assumed for the mean wind distribution. The extreme load with the recurrence period of 50 years is estimated based on the probability of exceedance of the load.

First, the uncertainty of the extrapolated extreme load based on the numeral simulations is discussed and a new convergence criterion is proposed in “A new convergence criterion” section. A new extrapolation factor is then proposed to predict maximum tower bending moments in “A new convergence criterion” section. Finally, empirical formulae to estimate the expected value of maximum tower moment are proposed in “Empirical formulae for the expected maximum tower load estimation” section.

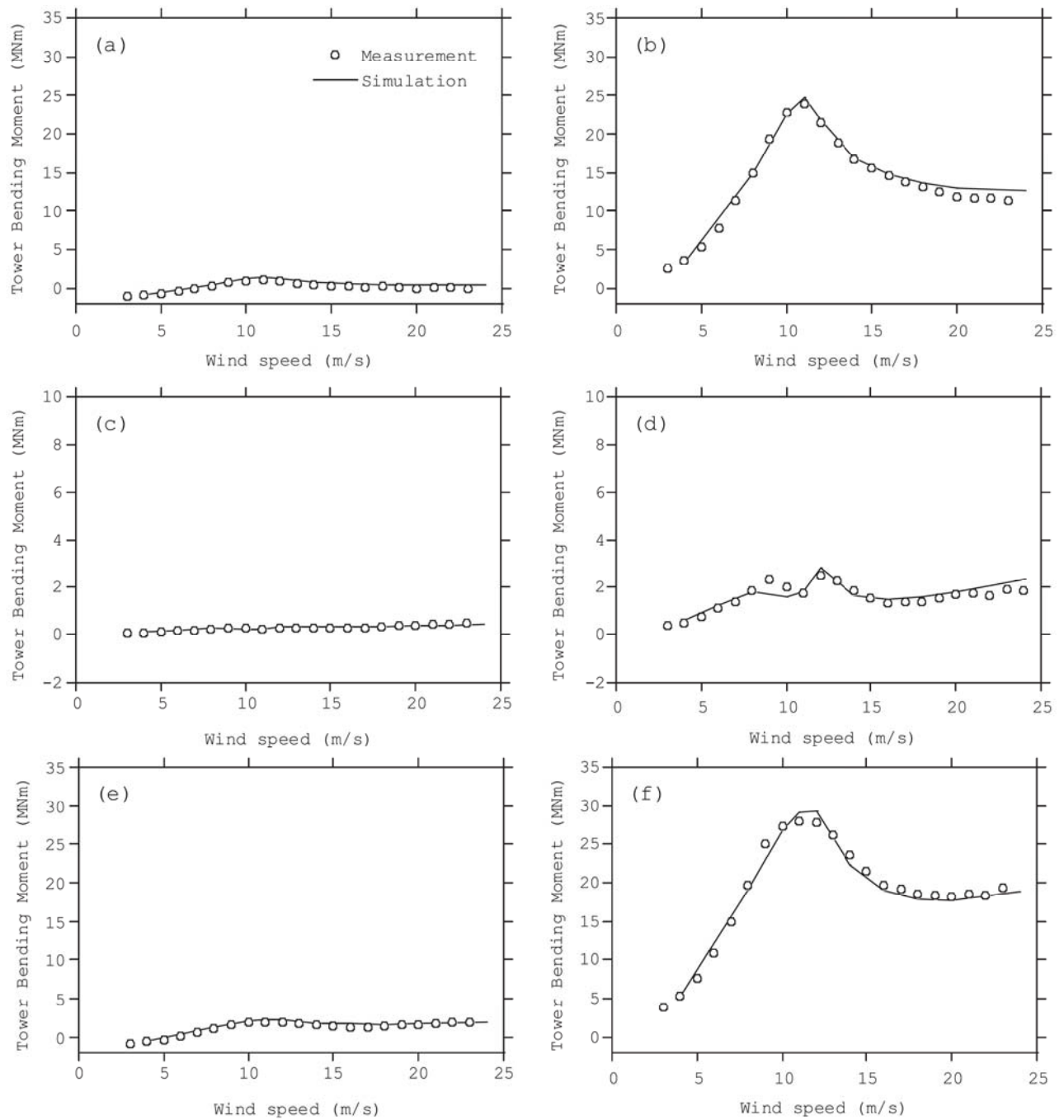


Figure 4. Fore-aft tower bending moment: (a) mean at 73.1 m, (b) mean at 10.9 m, (c) standard deviation at 73.1 m, (d) standard deviation at 10.9 m, (e) maximum at 73.1 m, and (f) maximum at 10.9 m.

A new convergence criterion

As specified in IEC61400-1, the extreme load is usually extrapolated from maximum loads of limited number of simulations by fitting the simulated maximum loads to three-parameter Weibull distribution. To reduce the uncertainty of the extrapolation, a criterion proposed by Fogle et al. (2008) is typically used. Figure 5(a) shows the example of the simulated maximum fore-aft tower base bending moment that satisfies the criteria and the fitted distribution for $I_{\text{ref}} = 12\%$ and hub-height wind speed of 16 m/s. Figure 6(a) shows the set of the estimated extreme load estimated from set of simulated maximum load, which satisfies the conventional criteria for $I_{\text{ref}} = 12\%$ and

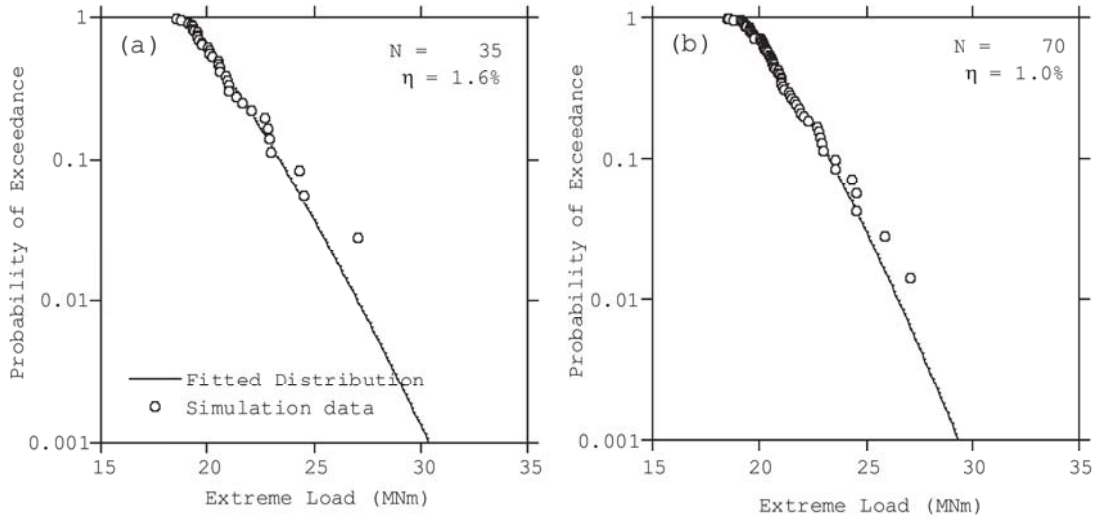


Figure 5. Probability distribution of maximum fore-aft tower base bending moment: (a) conventional criteria and (b) proposed criteria for $I_{ref} = 12\%$ and $u = 16$ m/s.

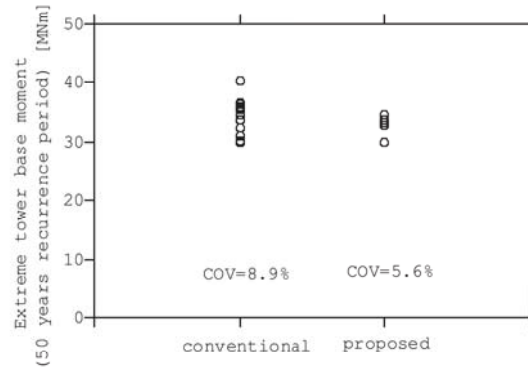


Figure 6. Estimated extreme tower base fore-aft bending moment during power production by using different data sets that satisfy the conventional and proposed criteria.

$\bar{U} = 10$ m/s. In this case, the coefficient of variation (COV) of the extreme value is 8.9%, which is larger than the assumed value in IEC61400-1 to derive the partial safety factor for the normal conditions as mentioned by Tarp-Johansen et al. (2002).

In addition to these criteria, more strict criteria are proposed to reduce the uncertainty in this study. Proposed convergence criteria are expressed in terms of relative error η , which is the ratio of the error E and S_{ave} , see equations (2)–(4). The error is the sum of all the difference between the simulation and the fitted distribution

$$\eta = \frac{E}{S_{ave}} \quad (2)$$

$$E = \sqrt{\sum_{j=1}^N \frac{(s_{simj} - s_{fitj})^2}{N}} \quad (3)$$

$$s_{ave} = \max \left(\frac{1}{N} \sum_{j=1}^N s_{xj}; \text{cut-in} \leq x \leq \text{cut-out} \right) \quad (4)$$

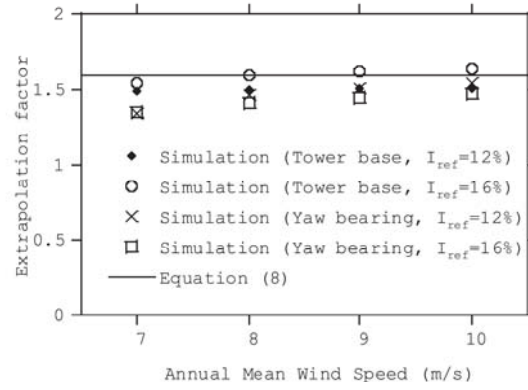


Figure 7. Proposed new extrapolation factor g_{ext} for fore-aft bending moment.

In the proposed criteria, the relative error is limited depending on the turbulence intensity as shown in equation (5)

$$\eta \leq 1.25I_{\text{ref}} \quad (5)$$

Figure 5(b) shows the probability distribution of the estimated extreme load from set of simulations, which satisfies the proposed criteria. The outliers of the data decrease by using the proposed criteria. Figure 6 presents the set of the estimated extreme load. The COV of the extreme value estimated from set of simulated maximum load that satisfies the proposed criteria decreases to 5.6%, which is closer to the assumed COV in IEC61400-1 for the partial safety factor of extreme load in the study by Tarp-Johansen et al. (2002).

A new extrapolation factor

C_{ext} is used to estimate the extreme load with the recurrence period of 50 years M_{50} as

$$M_{50} = C_{\text{ext}}M'_{\text{max}} \quad (6)$$

where M'_{max} is the maximum of the expected maximum load $M_{\text{max}}(u)$, that is, the maximum of the average of the 10-min maximum load for different wind speed ($M'_{\text{max}} = \max(M_{\text{max}}(u))$). However, the ratio of M_{50} and M'_{max} may vary depending on the component as mentioned by Moriarty (2008).

In this study, a new *extrapolation factor*, g_{ext} , is proposed and is defined for the load subtracted by the mean value. By using the extrapolation factor g_{ext} , the extreme load is estimated by

$$M_{50} = g_{\text{ext}}(M'_{\text{max}} - \bar{M}) + \bar{M} \quad (7)$$

where \bar{M} is the mean value of the load for the wind speed where M'_{max} occurs.

The extreme fore-aft moment at the top and bottom of the tower is calculated for different annual mean wind speed and different turbulence intensity by using the extrapolation with the criteria proposed in the previous section, and the ratio between $M_{50} - \bar{M}$ and $M'_{\text{max}} - \bar{M}$, which corresponds to the extrapolation factor, is calculated and plotted in Figure 7. This ratio does not depend on turbulence intensity, the component, or annual mean wind speed, which implies a constant value may be used as the extrapolation factor. In this study, following value is proposed

$$g_{\text{ext}} = 1.6 \quad (8)$$

The extrapolation coefficient C_{ext} can be derived from equations (6) and (7) by using the extrapolation factor g_{ext} as

$$C_{\text{ext}} = \frac{M_{50}}{M'_{\text{max}}} = \frac{g_{\text{ext}}(M'_{\text{max}} - \bar{M}) + \bar{M}}{M'_{\text{max}}} \quad (9)$$

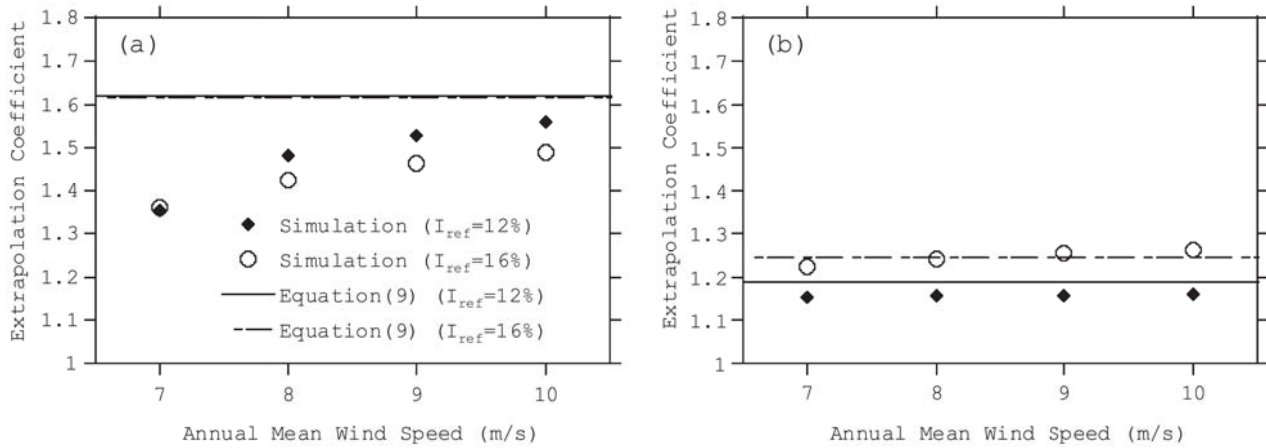


Figure 8. Proposed and simulated extrapolation coefficients for (a) yaw bearing fore-aft moment and (b) tower bottom fore-aft moment.

Figure 8 shows the ratio of the extreme value of the fore-aft bending moment and the maximum of the expected maximum fore-aft bending moment together with the proposed extrapolation coefficient as shown in equation (9). The extrapolation coefficient differs considerably depending on the turbulence intensity and the position of the tower. Clearly, the extrapolation coefficient for the yaw bearing fore-aft moment exceeds 1.5, while the extrapolation coefficient for the tower bottom fore-aft moment is about 1.2. The extrapolation coefficient at the tower bottom decreases since the mean value increases, and this change is well estimated by equation (9).

Empirical formulae for the expected maximum tower load estimation

In Japan, the actual wind conditions at site are quite different from those specified in IEC class. For this reason, the owner has to complete the assessment of structural integrity based on the site wind condition. The extreme wind event with a 50-year return period in the idling and standing still conditions can be accurately estimated by using an equivalent static wind load evaluation considering non-Gaussian assumption (Binh et al., 2009). However, the wind loads is affected by the pitch control under operating condition. Therefore, the wind load cannot be explained by the conventional quasi-static theory.

Ishii and Ishihara (2010) proposed an empirical model for the estimation of the expected value of the fore-aft tower bending moment assuming that fore-aft bending moment on a wind turbine tower is caused by the thrust force acting on the rotor and the drag forces acting on the tower and the nacelle only. However, the moment on the rotor plane and the gravity force of nacelle also leads to the fore-aft bending moment on the wind turbine tower as shown in Figure 9. The offset of the center of gravity of the nacelle causes tower bending moment. The rotor moment is caused by the weight of the rotor itself and wind shear, that is, the difference in the wind speed at the upper tip and the lower tip of the rotor.

Figure 10 shows the cause of the fore-aft tower bending moment for two different wind speeds at all the heights of tower. It is clear that at the tower base, the main cause of the fore-aft moment is the thrust force. However, at the tower top, this is not the case. In summary, the tower bending moment during power production $M(u)$ can be expressed as a summation of the moment caused by the thrust force and drag force on the nacelle and the tower $M_{DT}(u)$, rotor moment $M_R(u)$, and gravity force M_g

$$M(u) = M_{DT}(u) + M_R(u) + M_g \quad (10)$$

Each term in equation (10) is separated into mean component and fluctuating component. In this study, the fluctuating component of the tower moment caused by thrust and drag ($\sigma_{DT}(u)$), and rotor moment ($\sigma_R(u)$) are considered separately and they are assumed to have no correlations. This assumption can be justified because the thrust force is caused by the average wind speed on the rotor, whereas the rotor moment is caused by the shear of the wind speed, and it is reasonable to assume they are independent. Thus, the expected value of maximum tower

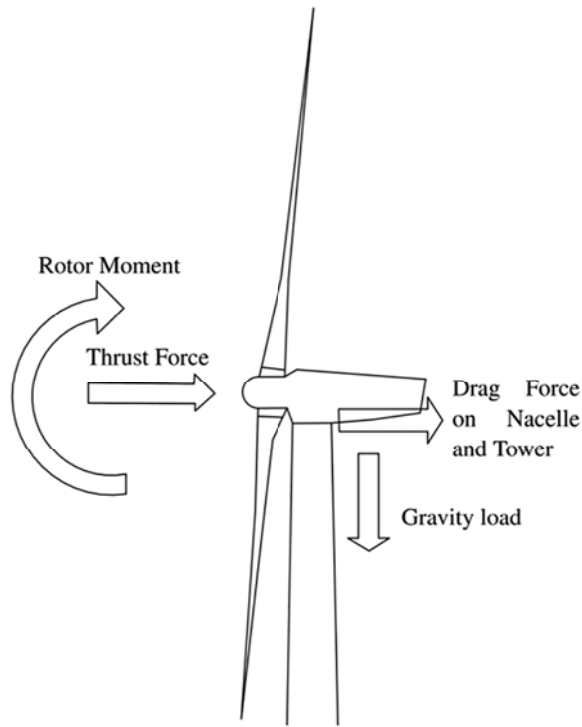


Figure 9. Scheme of the forces acting on the wind turbine rotor, nacelle, and tower in the fore-aft direction.

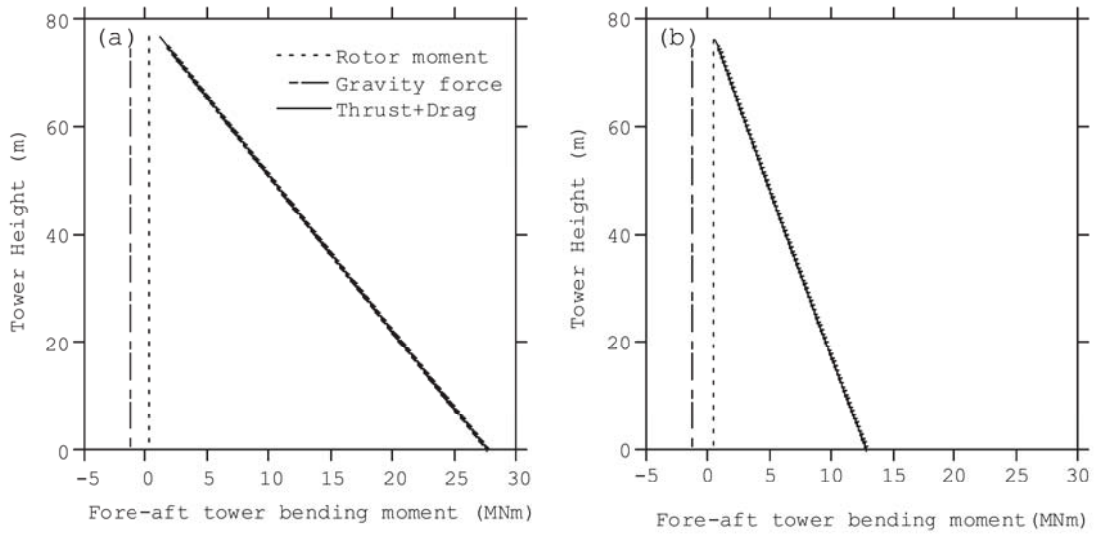


Figure 10. Cause of tower bending moment at different heights of the tower: (a) $u = 13$ m/s and (b) $u = 18$ m/s.

fore-aft bending moment M_{\max} can be estimated by equation (12). Note that gravity force does not have any fluctuating component

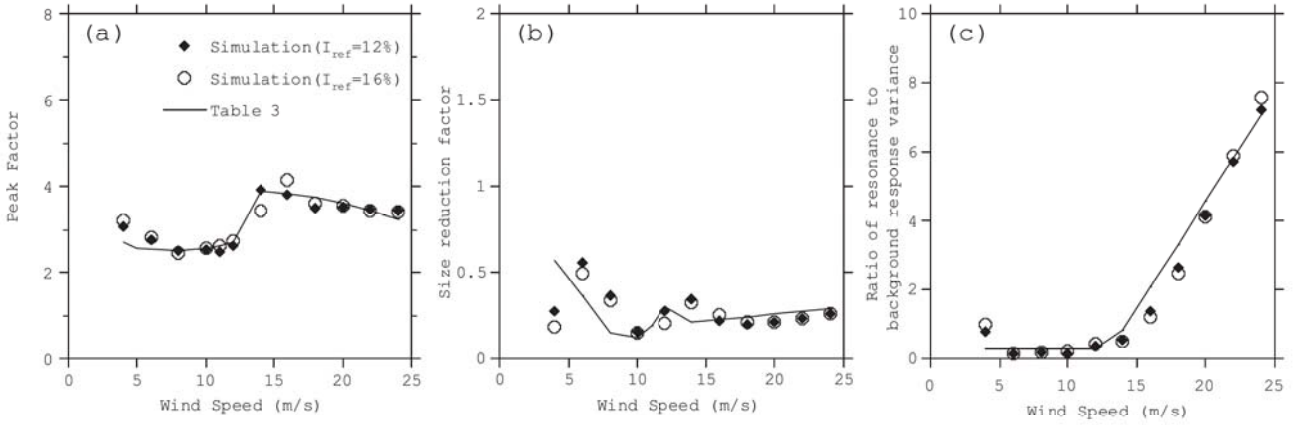
$$\bar{M}(u) = \overline{M_{DT}}(u) + \overline{M_R}(u) + M_g \quad (11)$$

$$M_{\max}(u) = \bar{M}(u) + \sqrt{(g_{DT}(u)\sigma_{DT}(u))^2 + (g_R(u)\sigma_R(u))^2} \quad (12)$$

Table 3. Empirical formulae for $g_{DT}(u)$, $K_{DT}(u)$, and $R_{DT}(u)$ as functions of hub-height wind speed u .

	Below-rated wind speed	Above-rated wind speed
$g_{DT}(u)$	$-0.3 \sin\left(\pi \cdot \frac{V_{in} - u}{V_{in} - V_r}\right) + 2.8$	$1.1 \cos\left(0.4\pi \cdot \frac{u - V_r}{V_{out} - V_r}\right) + 2.8$
$K_{DT}(u)$	$0.25 \cos\left(1.6\pi \cdot \frac{V_{in} - u}{V_{in} - V_r}\right) + 0.35$	$0.1 \cdot \left(\frac{u - V_r}{V_{out} - V_r}\right) + 0.2$
$R_{DT}(u)$	0.3	$7.5 \cdot \left(\frac{u - V_r}{V_{out} - V_r}\right) + 0.2$

V_{in} : cut-in wind speed (m/s); V_{out} : cut-out wind speed (m/s); V_r : rated wind speed (m/s).

**Figure 11.** Parameters to estimate the fore-aft tower bending moment caused by thrust and drag forces: (a) peak factor $g_{DT}(u)$, (b) size reduction factor $K_{DT}(u)$, and (c) ratio of resonance to background response variance $R_{DT}(u)$.

Here, $\bar{M}(u)$ is the mean fore-aft tower bending moment, $\bar{M}_{DT}(u)$ and $\bar{M}_R(u)$ are the mean fore-aft tower moment caused by thrust force and drag force, and rotor moment, respectively. M_g is the tower moment caused by the gravity force and $g_{DT}(u)$ and $g_R(u)$ are the peak factor of the fore-aft tower base moment caused by the thrust and drag, and rotor moment, respectively.

First, $\bar{M}_{DT}(u)$, $g_{DT}(u)$, and $\sigma_{DT}(u)$ are discussed. The fore-aft tower bending moment at the height of h caused by thrust and drag $\bar{M}_{DT}(u)$ can be calculated as follows

$$\begin{aligned} \bar{M}_{DT}(u) = & \frac{1}{2} \rho u^2 C_T(u) \pi R^2 \times (H_h - h) \\ & + \left(\frac{1}{2} \rho u^2 C_{DN} A_N \right) (H_h - h) + \int_h^{H_t} \frac{1}{2} \rho u(z)^2 C_{DT} d(z) (z - h) dz \end{aligned} \quad (13)$$

Here, H_h is the hub height, u is the wind speed at hub height, H_t is the height of the tower, C_{DN} is the drag coefficient of the nacelle, C_{DT} is the drag coefficient of the tower, A_N is the area of the nacelle, $C_T(u)$ is the thrust coefficient, and $u(z)$ and $d(z)$ are the wind speed and diameter of the tower at the height z .

The standard deviation of thrust and drag $\sigma_{DT}(u)$ can be expressed as follows by using the turbulence intensity I_1 , the size reduction factor $K_{DT}(u)$, and the ratio of resonance to background response variance $R_{DT}(u)$

$$\sigma_{DT}(u) = 2I_1 \sqrt{K_{DT}(u)} \sqrt{(1 + R_{DT}(u)) \cdot \bar{M}_{DT}(u)} \quad (14)$$

In this study, empirical formulae for these parameters are proposed as shown in Table 3. The proposed formulae are derived empirically as to fit the values based on simulations. Figure 11 shows the comparison of the simulation and the proposed empirical formulae for peak factor, size reduction factor and the ratio of the resonance to the background response variance. Proposed models show good agreements with the simulations.

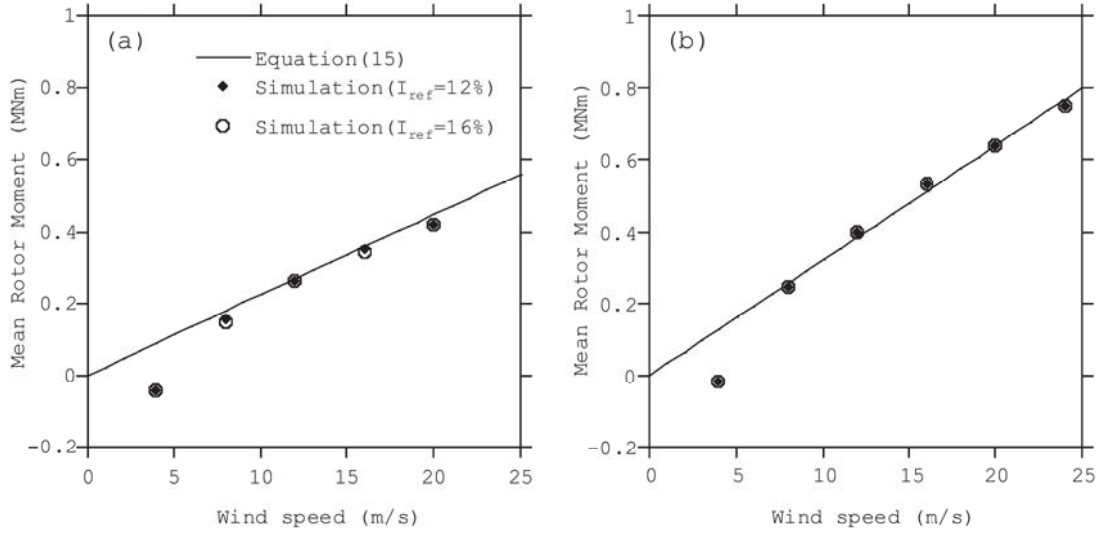


Figure 12. Mean rotor moment: (a) $\alpha = 0.14$ and (b) $\alpha = 0.20$.

Then, the parameters related to the rotor moment, $\overline{M}_R(u)$, $g_R(u)$ and $\sigma_R(u)$, are discussed. The moment on the rotor plane is caused by the wind shear. To understand how the mean rotor moment changes with wind speed and shear, numerical simulations with different wind speed and shear are carried out and mean rotor moment is plotted in Figure 12. The mean rotor moment is a function of the shear exponent and wind speed but does not depend on turbulence intensity. In this study, the mean rotor moment $\overline{M}_R(u)$ in (N m) is modeled by using following equation

$$\overline{M}_R(u) = 0.193 \alpha u D^3 \quad (15)$$

Here, α is the shear exponent, u is the mean wind speed at hub height in m/s, and D is the diameter of the rotor in m. Predicted mean rotor moment by using equation (15) is also plotted in Figure 12. The mean rotor moments by proposed formula show good agreements with those from the dynamic simulations for above-rated wind speeds, and the underestimation near the cut-in wind speeds is not important for estimating the maximum bending moment.

The fluctuating component (standard deviation) of the rotor bending moment $\sigma_R(u)$ can be modeled by using the root mean square of the moment on the rotor $\text{RMS}_R(u)$, which is defined by

$$[\sigma_R(u)]^2 = [\text{RMS}_R(u)]^2 - [\overline{M}_R(u)]^2 \quad (16)$$

The root mean square of the rotor moment for different wind shear, different turbulence intensity, and different wind speed is plotted in Figure 13. It is clear that unlike its mean, the fluctuating component is not only the function of wind shear and wind speed, but also the function of turbulence intensity. In this study, the RMS_R in (N m) is modeled by using following equation. Predicted root mean square (RMS) of the rotor moment by using equation (17) is also plotted in Figure 13

$$\text{RMS}_R(u) = (2.047\alpha + 0.963)(0.5I_{\text{ref}} + 0.03)u^{0.7}D^3 \quad (17)$$

The peak factor is defined as the ratio of maximum value subtracted by mean value, and standard deviation

$$g_R(u) = \frac{M_{R\text{max}}(u) - \overline{M}_R(u)}{\sigma_R(u)} \quad (18)$$

The peak factors are calculated for all the cases and plotted in Figure 14, which indicates that an uniform peak factor can be used for all the cases. Therefore, the peak factor is assumed to be 3.5 for all the hub-height wind speeds

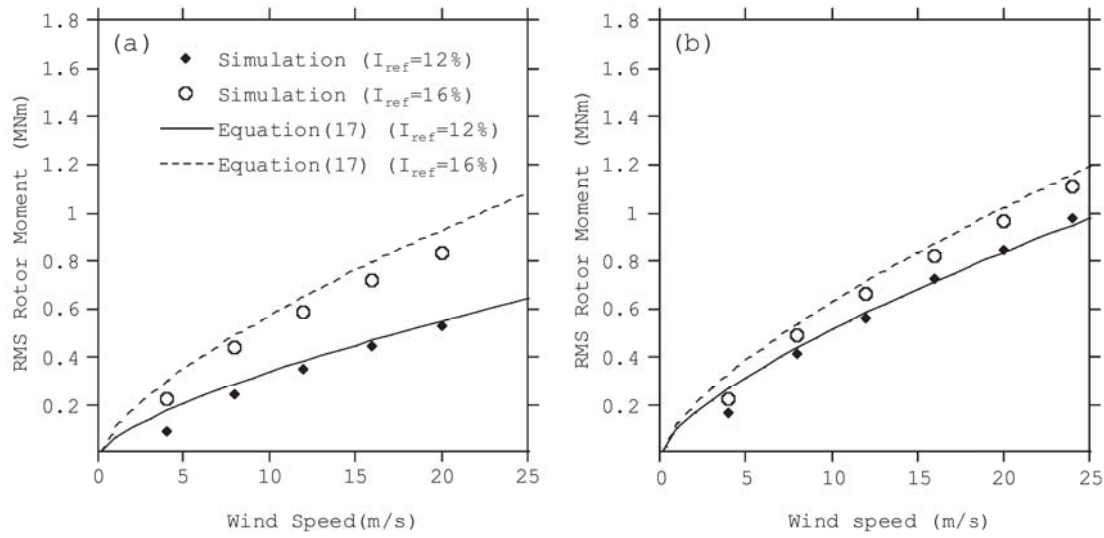


Figure 13. RMS of rotor moment: (a) $\alpha = 0.14$ and (b) $\alpha = 0.20$.

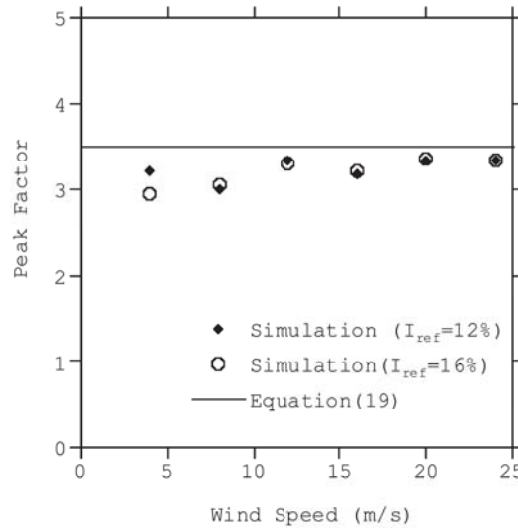


Figure 14. Peak factor for rotor moment.

$$g_R(u) = 3.5 \quad (19)$$

Finally, numerically simulated fore-aft tower moment and estimated value by using the proposed equations (11) and (12) are compared and shown in Figure 15. The proposed model shows good agreement with the simulations for all the cases.

Conclusion

In this study, a numerical model of a wind turbine is developed and dynamic simulations are carried out to investigate the extreme wind load on the wind turbine tower during power production. Following conclusions were obtained.

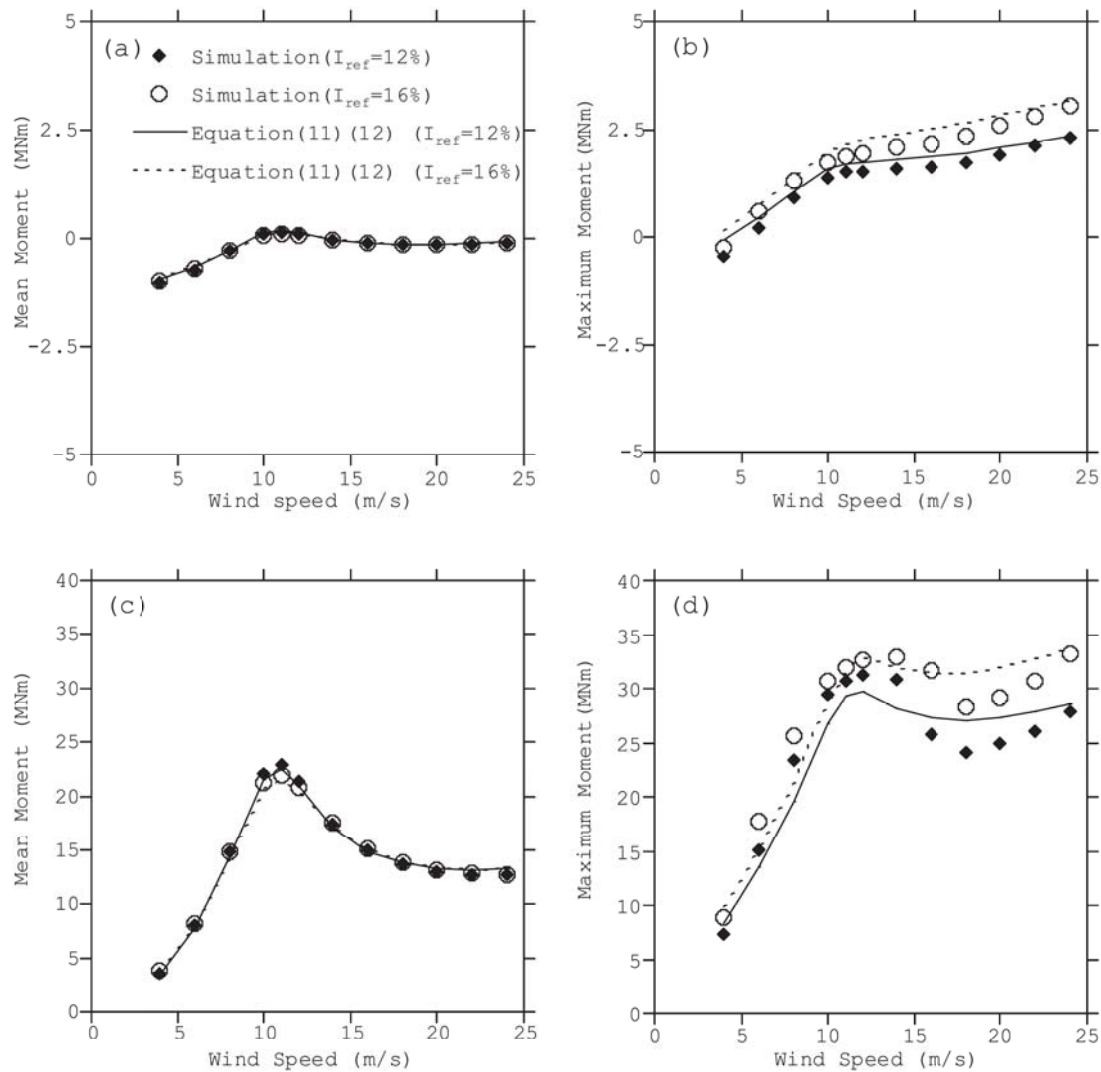


Figure 15. Fore-aft bending moment: (a) mean at yaw bearing, (b) expected maximum at yaw bearing, (c) mean at tower bottom, and (d) expected maximum at tower base.

1. A new criterion is proposed for the data sets to be used for the statistical extrapolation. The resulting uncertainty satisfies the requirement in the standard for prediction of wind load.
2. A new extrapolation factor is proposed by subtracting the mean value. The predicted extreme loads during power production at all the heights of the tower show good agreement with the measurement.
3. The expected value of 10-min maximum tower bending moment by the proposed empirical formulae, which includes the effect of drag forces on the tower and the nacelle, thrust force, rotor moment and gravity force, shows good agreement with the simulation results.

Acknowledgements

The on-site measurement was carried out in cooperation with Tokyo Electric Power Company (TEPCO) and Kajima Corporation. The authors wish to express their deepest gratitude to the concerned parties for their assistance during this study.


Declaration of conflicting interests

The author(s) declared no potential conflicts of interest with respect to the research, authorship, and/or publication of this article.

Funding

The author(s) disclosed receipt of the following financial support for the research, authorship, and/or publication of this article: This study is carried out as a part of “Offshore Wind Power Generation System Proving Research” funded by New Energy and Industrial Technology Development Organization (NEDO) Japan and Tokyo Electric Power Company (TEPCO).

ORCID iD

Atsushi Yamaguchi  <https://orcid.org/0000-0002-8749-5215>

References

- Binh LV, Ishihara T, Phuc PV, et al. (2009) A peak factor for non-Gaussian response analysis of wind turbine tower. *Journal of Wind Engineering and Industrial Aerodynamics* 96(10–11): 2217–2227.
- DNV-GL (2010) *Bladed Theory Manual: Version 4.1*. DNV-GL.
- Fogle J, Agarwal P and Manuel L (2008) Towards an improves understanding of statistical extrapolation for wind turbine extreme loads. In: *46th AIAA aerospace sciences meeting and exhibition*, Reno, NV, 7–10 January.
- Fukumoto Y, Ishihara T, Yamaguchi A, et al. (2013) Current state of research activity on bottom mounted offshore wind turbine in Japan. In: *EWEA offshore*, Frankfurt, 19–21 November.
- IEC61400-1:2005 + AMD1: 2010 (2010) Wind turbines—part 1: Design requirements.
- T Ishihara (ed.) (2010) *Guidelines for Design of Wind Turbine Support Structures and Foundation*. Tokyo, Japan: Japan Society of Civil Engineers (in Japanese).
- Ishii H and Ishihara T (2010) Numerical study of maximum wind load on wind turbine towers under operating conditions. In: *Fifth international symposium on computational wind engineering*, Chapel Hill, NC, 23–27 May.
- Moriarty PJ (2008) Database for validation of design load extrapolation techniques. *Wind Energy* 11(6): 559–576.
- Oh S and Ishihara T (2018) Structural parameter identification of a 2.4MW bottom Fixed wind turbine by excitation test using an active mass damper. *Wind Energy* 21(11): 1232–1238.
- Okubo K, Yamamoto M, Fukumoto Y, et al. (2016) Wind loads on a bottom-mounted offshore wind turbine tower. In: *First international symposium on flutter and its application*, Tokyo, Japan, 15–17 May.
- Tarp-Johansen NJ, Madsen PH and Frandsen S (2002) *Partial Safety Factors for Extreme Load Effects*. Roskilde: Risø National Laboratory.
- Yoshida S (2011) Variable-speed variable pitch control for aero-servo-elastic simulations of wind turbine support structures. *Journal of Fluid Science and Technology* 6(3): 300–312.